

Subcritical bifurcation in spatially extended systems

This content has been downloaded from IOPscience. Please scroll down to see the full text.

2012 Nonlinearity 25 761

(<http://iopscience.iop.org/0951-7715/25/3/761>)

View [the table of contents for this issue](#), or go to the [journal homepage](#) for more

Download details:

IP Address: 144.214.75.230

This content was downloaded on 07/03/2014 at 02:27

Please note that [terms and conditions apply](#).

Subcritical bifurcation in spatially extended systems

Weinan E^{1,2}, Xiang Zhou³ and Xiuyuan Cheng²

¹ Department of Mathematics, Princeton University, Princeton, NJ 08544-1000, USA

² Program in Applied and Computational Mathematics, Princeton University, Princeton, NJ 08544-1000, USA

³ Division of Applied Mathematics, Brown University, Providence, RI 02912, USA

E-mail: weinan@math.princeton.edu

Received 10 June 2011, in final form 17 January 2012

Published 13 February 2012

Online at stacks.iop.org/Non/25/761

Recommended by B Eckhardt

Abstract

A theory for noise-driven subcritical instabilities in spatially extended systems is put forward. The theory allows one to calculate the critical bifurcation parameter for a first-order phase transition in such non-equilibrium systems in the thermodynamic limit and analyse the mechanism of phase transition. Two examples with distinctive features are studied in detail to demonstrate the usefulness of the theory and the different scenarios that can occur in the thermodynamic limit of non-equilibrium systems.

Mathematics Subject Classification: 60H30, 82C26

(Some figures may appear in colour only in the online journal)

1. Introduction

Many important physical systems exhibit subcritical bifurcations. One of the best known examples is laminar flow in a circular pipe, which is linearly stable for all Reynolds number, yet it undergoes transition to more complicated and eventually turbulent flows when the Reynolds number is sufficiently large [1, 2]. In contrast to supercritical instabilities which are local phenomena in the configuration space and can be studied by analysing linearized models, subcritical instabilities are consequences of the global behaviour of the system under consideration.

It is clear that finite amplitude perturbations are needed in order to trigger subcritical instabilities. What is not clear, however, is how to turn this intuition into a set of tools with which one can analyse subcritical instabilities and make quantitative predictions. In this paper, we are interested in subcritical instabilities driven by vanishingly small amplitude noise. In this case, it is well known that if a system has finite degrees of freedom, it will simply wander around in the configuration space, moving from one basin of attraction to another over

exponentially long time scales (in terms of the noise amplitude). Even though the system will in general spend different amount of time near different stable states, all the stable states will be visited during the course of the dynamics, assuming that the noise-driven dynamics is ergodic, a property that generally holds for systems forced by white noise. For this reason, there are only quantitative differences between different stable states. For spatially extended systems, however, a simplification might occur, namely all but one stable states are effectively suppressed for most values of the system parameters. At some particular parameter values, the selected stable state will change suddenly, and these are the points of phase transition for the system. We will provide quantitative methods for determining the bifurcation points and studying the stability properties of the different states under noisy perturbations, and we will investigate some canonical examples.

It is natural to draw an analogy with phase transition in equilibrium systems: subcritical bifurcation is a lot like first-order phase transition, whereas supercritical bifurcation is a lot like second-order phase transition [3]. For thermodynamic phase transition, the system is described by a free energy, and the stable states are local minima of the free energy. The lower the free energy, the more stable the state is. In addition, the following statements are generally true for first-order phase transition [4]:

- (i) In noise-induced transition from a less stable state to a more stable state, the size of the critical nucleus is effectively finite. For a large system with volume V , the probability for a less stable state to survive in the presence of thermal noise is proportional to α^V for some number $\alpha < 1$. Therefore only the state with the lowest free energy survives in the thermodynamic limit.
- (ii) If we place two states next to each other, the state with lower free energy will propagate into the higher energy state. Furthermore, this propagation is described asymptotically by a travelling wave. The speed of the travelling wave depends on the difference between the energies of the two states.
- (iii) The mechanism of transition from a less stable state to a more stable state is that of nucleation and propagation: due to the noise, droplets of the new phase are continuously nucleated. Most of these droplets cannot survive. But if a droplet reaches a critical size, it will spread out and propagate into the territory occupied by the old phase.

In terms of the stochastic dynamical system:

$$dX_t = b(X_t) dt + \sigma dW_t,$$

where dW_t is the Gaussian white noise, the dynamics of equilibrium systems are represented by that of gradient systems, i.e. $b(x) = -\nabla V(x)$ for some energy function V and the noise is additive (σ is a constant). In this paper we are primarily interested in non-gradient systems, i.e. b is not the gradient of a function or the noise is multiplicative. A canonical example of non-gradient systems is the dynamics of viscous fluids. We are interested in the following question: to what extent the picture described above still holds for non-gradient systems, and which quantities replace the free energy difference as a criteria for comparing the stability of two states? These questions will be answered in the context of noise-driven systems with the help of the large deviation theory.

Below when we mention ‘locally stable states’, we mean linearly stable states (or sets) of the unperturbed system. We will limit ourselves to the situation when the homogeneous system has only two locally stable states. We will focus primarily on the competition between the two locally stable homogeneous states over large (infinite) domains. Extension to more complex situations will be discussed in future work.

Two ideas have been proposed in the literature to study the relative stability of two states. One is to look the nucleation process: if critical nucleus of state A is compact within the

background of state B , then the state A is more stable than state B . The other [3, 5, 6] is to look at the dynamics of the system when state A and B are placed against each other: if A invades B asymptotically, then A is more stable than B . While both seem like very natural ideas, we will show that they are inadequate in general. The right way to handle general situations is to consider the action, a concept coming from large deviation theory, which, roughly speaking, measures the amount of noise needed in order to make a transition from one state to another.

Unlike thermodynamic variables for equilibrium systems which depend only on the state of the system, action depends on the path and is a function of both the initial and final states of the system. This may very well be a general phenomenon for non-equilibrium systems.

2. Review of the large deviation theory

We start with an introduction of the large deviation theory in a finite-dimensional setting [7]. A more physical presentation of large deviation theory can be found in [8].

We consider a random process $X_t = X(t) : \mathbb{R}_+ \rightarrow \mathbb{R}^d$ defined by the following (Ito) stochastic ordinary differential equation (SODE):

$$dX_t = b(X_t) dt + \sqrt{\varepsilon} \sigma(X_t) dW_t, \tag{2.1}$$

where W_t is a standard Wiener process in \mathbb{R}^d . The noise amplitude ε is a small parameter and we are concerned with the zero noise limit $\varepsilon \downarrow 0$. Let $\varphi(\cdot)$ be an absolutely continuous function defined on $[0, T]$. The Freidlin–Wentzell theory [7, 9] tells us that the probability for $X(\cdot)$ to stay in the δ -tube around φ on the time interval $[0, T]$ is

$$\mathbb{P}(\rho(X, \varphi) < \delta) \asymp \exp\left(-\frac{1}{\varepsilon} S_T(\varphi)\right), \tag{2.2}$$

where $\rho(\varphi_1, \varphi_2) = \sup_{t \in [0, T]} |\varphi_1(t) - \varphi_2(t)|$, and $S_T(\varphi)$ is the Freidlin–Wentzell action functional of φ on the time interval $[0, T]$, defined as

$$S_T(\varphi) = \frac{1}{2} \int_0^T \|\dot{\varphi} - b(\varphi)\|_{A(\varphi(t))}^2 dt, \tag{2.3}$$

if the integral exists, otherwise $S_T(\varphi) := +\infty$. Here the matrix-valued function $A(\cdot)$ is defined by $A(x) := \sigma(x)\sigma(x)^T$ and for any positive definite matrix A , the norm $\|\cdot\|_A$ is defined as $\|z\|_A := \langle z, A^{-1}z \rangle$ for any $z \in \mathbb{R}^d$.

A key quantity derived from the large deviation principle is the cost function

$$W(x, y, t) = \inf_{\varphi \in C([0, t]): \varphi(0)=x, \varphi(t)=y} S_t(\varphi). \tag{2.4}$$

Let

$$W(x, y) = \inf_{t>0} W(x, y, t). \tag{2.5}$$

Heuristically, $W(x, y)$ is the minimum cost of forcing system (2.1) to end at the state y if it is initiated at the state x . One can also define a cost function associated with two sets A, B : $W(A, B) = \inf_{x \in A, y \in B} W(x, y)$. For a given stable state x , the function $W_x(\cdot) := W(x, \cdot)$ is called the *quasi-potential* [7] associated with the state x . In gradient systems where $b(x) = -\nabla V(x)$ for some function V and $\sigma = 1$, $W_x(y) = 2(V(y) - V(x))$. Here the factor of 2 is due to the fact that we write the amplitude of noise in (2.1) as $\sqrt{\varepsilon}$, instead of $\sqrt{2\varepsilon}$ as in the conventional physical literature.

Freidlin–Wentzell theory generalizes naturally to stochastic partial differential equations (SPDE). This is done for the example of the stochastically perturbed Allen–Cahn equation in [10] and [11, 12]. Consider a SPDE in the form

$$\frac{\partial \mathbf{u}}{\partial t} = \delta \Delta \mathbf{u} + \delta^{-1} \mathbf{f}(\mathbf{u}) + \sqrt{\varepsilon} \boldsymbol{\eta}, \quad x \in \Omega \subset \mathbb{R}^d, \tag{2.6}$$

where $\mathbf{u}(x, t) \in \mathbb{R}^n$, $\delta > 0$, $0 < \varepsilon \ll 1$, $\mathbf{f} : \mathbb{R}^n \rightarrow \mathbb{R}^n$ is the nonlinear term. We put a small parameter δ here but keep the domain Ω fixed purely for notational convenience. It is obvious that after rescaling, small values of δ correspond to large spatial domains. In our numerical examples presented below, we typically fix the domain size to be 1 and use very small values of δ . The spatial-temporal noise $\boldsymbol{\eta}$ in the SPDE (2.6) has zero mean and spatial correlation given by an operator \mathbf{K} ,

$$\mathbb{E}[\boldsymbol{\eta}(x, t)\boldsymbol{\eta}(y, s)] = \mathbf{K}(x, y)\delta(t - s).$$

The action functional for a path $\mathbf{u}(x, t) : \Omega \times \mathbb{R}_+ \rightarrow \mathbb{R}^n$ in this infinite-dimensional setting is [13]

$$S_T[\mathbf{u}] = \frac{1}{2} \int_0^T dt \int_{\Omega} \int_{\Omega} \langle \mathcal{F}\mathbf{u}(x, t), \mathbf{K}^{-1}\mathcal{F}\mathbf{u}(y, t) \rangle dy dx, \quad (2.7)$$

where $\langle \cdot \rangle$ is the inner product in Euclidean space \mathbb{R}^d and here we define

$$\mathcal{F}\mathbf{u}(x, t) := \dot{\mathbf{u}}(x, t) - \delta\Delta\mathbf{u}(x, t) - \delta^{-1}\mathbf{f}(\mathbf{u}(x, t)), \quad (2.8)$$

($\dot{\mathbf{u}}$ is time derivative). If $\boldsymbol{\eta}$ is the white noise, the action functional is simplified to be

$$S_T[\mathbf{u}] = \frac{1}{2} \int_0^T dt \int_{\Omega} \|\dot{\mathbf{u}} - \delta\Delta\mathbf{u} - \delta^{-1}\mathbf{f}(\mathbf{u})\|^2 dx, \quad (2.9)$$

where $\|\cdot\|$ is the standard l^2 norm in \mathbb{R}^d .

The notion of cost function and quasi-potential can obviously be extended to the above infinite-dimensional setting:

$$W(\mathbf{u}_1, \mathbf{u}_2, t) = \inf_{\mathbf{u} \in C([0, t]): \mathbf{u}(0) = \mathbf{u}_1, \mathbf{u}(t) = \mathbf{u}_2} S_t[\mathbf{u}]. \quad (2.10)$$

We should note that the cost function and quasi-potential depend not only on the deterministic drift terms, but also on the noise, i.e. σ in (2.1) or \mathbf{K} in (2.6).

3. Criteria for stability and instability

Given two (homogeneous) states, \mathbf{u}_1 and \mathbf{u}_2 , both are stable against infinitesimally small perturbations, which state survives in a spatially extended system in the presence of a very small noise? Here we give three answers to this question. The first is based on the large deviation theory, by comparing the action needed to switch from one state to the other. This one is quite rigorous and is expected to be generally valid. But it depends on the details of the noise—and this is unpleasant. The second is more heuristic, based on the idea of which state wins eventually if the two states are placed next to each other in space. The third criterion is more restrictive but is helpful in cases where transition between the different stable states proceed via saddle points. It is based on examining the spatial structure of the saddle points. For gradient systems, all three criteria are equivalent to each other. We will see later that this is no longer the case for non-gradient systems, and only the first criterion is valid in general (figure 1).

3.1. The action criterion

For the first criterion, we ask which state has a higher survival probability in the presence of noise. Such a survival probability can be defined through the escape probability of the stochastically perturbed system from the basin of attraction of the state under consideration. This escape probability is proportional to $\exp(-Q/\varepsilon)$ where Q is a constant associated with

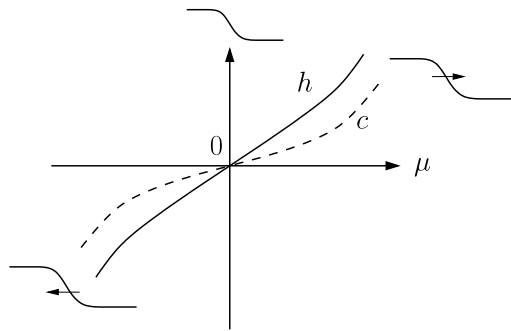


Figure 1. Illustration of the first two criteria in which we examine the escape action difference $h(u_1, u_2; \mu) := Q(u_1) - Q(u_2)$ and the speed of travelling wave going into u_2 , when the parameter μ varies. The arrows indicate the direction of the travelling wave connecting the two states.

the locally stable state. The mean exit time from the basin of attraction of the locally stable state is approximately $\exp(Q/\varepsilon)$.

According to large deviation theory [7], the quantity Q is the minimum value of the quasi-potential over the boundary of the basin of attraction of the locally stable state u :

$$Q(u) := \inf_{v \in \partial D(u)} W_u(v). \quad (3.1)$$

where $\partial D(u)$ is the boundary of the basin of attraction of the stable state u and W is the quasi-potential defined in section 2. For this reason, we will call the constant $Q(u)$ the *escape action* of the state u . For gradient systems where the nonlinear term in (2.6) is of the form $f = -\nabla_u V(u)$ for some function V , the total energy of system (2.6) is given by

$$E(u) = \frac{1}{2} \int_{\Omega} \delta \|\nabla u(x)\|^2 dx + \int_{\Omega} \delta^{-1} V(u) dx.$$

Thus, the escape action is the energy barrier $Q(u) = 2(E(u_s) - E(u))$ where u_s is the lowest energy saddle point next to u .

The concept of the escape energy is a generalization of the classical notion of activation energy. It bears some similarity to the work in [14–16] and [17–19].

The action criterion. The stability of a locally stable state depends on its escape action $Q(u)$. The higher the value of $Q(u)$, the more stable the state u is. For example, the state u_1 is more stable than u_2 if

$$h(u_1, u_2) := Q(u_1) - Q(u_2) > 0. \quad (3.2)$$

In the limit of infinite system size, if h approaches either $+\infty$ or $-\infty$, then only the more stable state with larger escape action survives, since the other states have zero survival probability. We will see below that for non-gradient systems, h may stay bounded as the system size goes to infinity. In this case, the two states co-exist.

3.2. The spatial competition criterion

A more heuristic criterion has been suggested in the literature [3, 5, 6]. In this criterion, the two states are placed next to each other, and one observes the long time behaviour of the system to see which state wins eventually.

The spatial competition criterion. We say that u_1 is more stable than u_2 if, with the initial condition described above, the state of the system converges to u_1 as $t \rightarrow +\infty$.

For a large class of systems, the state converges to a travelling wave under such initial conditions. Therefore the relative stability of the two states depends on the direction of the travelling wave.

This criteria has nothing to do with the noise, so it appears to be more intrinsic to the dynamics. However, as we will demonstrate below, it might depend on the details of the initial condition, i.e. how the two states are placed next to each other. In any case, we will see that this criterion does not necessarily give the right prediction.

It should be noted that for gradient systems, the two criteria are equivalent. In fact, in that case, $c \propto Q(u_1) - Q(u_2) = 2(V(u_2) - V(u_1))$, where c is the speed of the travelling wave going into the u_2 state [20].

3.3. The saddle point criterion

In many cases, the system escapes a basin of attraction through saddle points (for detailed discussion of this problem, refer to [7, 21–23]). If the relevant saddle point is a localized perturbation of the original state in physical space, then the survival probability of the original state is exponentially small as a function of the system size. In particular, the original state cannot survive in the thermodynamic limit. This is because that such a localized perturbation has a finite probability to occur, even though the probability might be small. In a large system, the probability that they never occur is exponentially small. Once they occur, they take over the whole system.

The saddle point criterion. Assume that u_s is a saddle point on the basins of attraction (in the phase space) of two neighbouring spatially homogeneous stable states u_1 and u_2 . If the difference $u_s - u_1$ decays at infinity in the physical space, then u_1 is less stable than u_2 .

Such a localized saddle point is usually referred to as the critical nucleus. Intuitively, the saddle point criterion says that if the critical nucleus going from u_1 to u_2 has finite size, then the state u_1 is less stable than u_2 . The saddle point criterion is also equivalent to the above two for gradient systems [20]. However, non-gradient systems does not have to escape a basin of attraction through saddle points, for example, when the basin boundary has no fixed points. It is also possible that there exist different nucleus which are localized with respect to the different homogeneous states u_1 and u_2 . We refer to section 5 for such example. Therefore this criterion is not universal either.

4. An example of nucleation and propagation

Consider

$$\begin{aligned} \frac{\partial u}{\partial t} &= \delta \Delta u + \delta^{-1} f(u, v), \\ \frac{\partial v}{\partial t} &= \delta \Delta v + \delta^{-1} g(u, v), \end{aligned} \quad (4.1)$$

where

$$\begin{aligned} f(u, v) &= (u - u^3 + \frac{6}{5})v + \frac{1}{2}\mu u, \\ g(u, v) &= \frac{1}{2}u^2 - v. \end{aligned} \quad (4.2)$$

Here μ is the bifurcation parameter. The base state $\mathbf{0} = (0, 0)$ is always a fixed point for all μ . We will examine the stability of the base solution as μ changes. Linear stability analysis shows

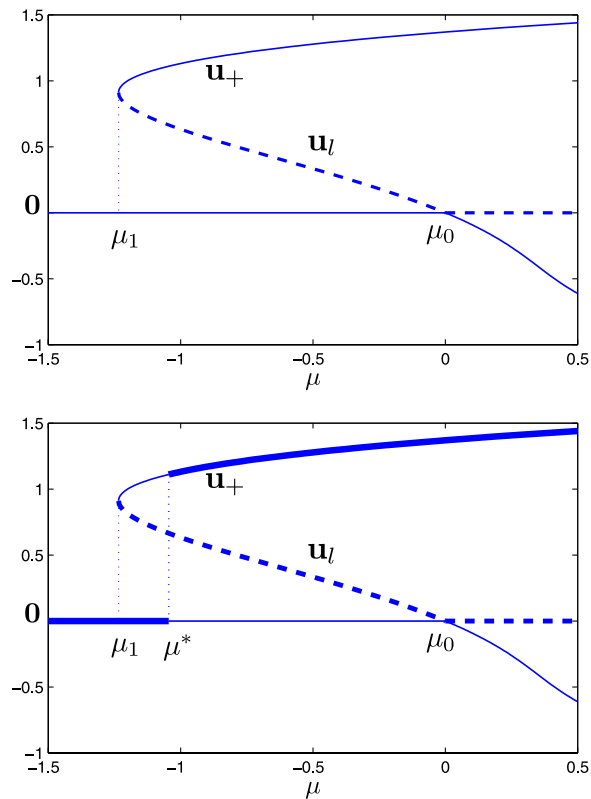


Figure 2. Bifurcation diagram of system (4.2). Only the graphs of the u -component of the fixed points are shown. The solid curves are linearly stable solutions, the dashed curves are linearly unstable solutions. A transcritical bifurcation and a subcritical bifurcation occur at $\mu_0 = 0$ and $\mu_1 \approx -1.2344$, respectively. In the lower figure, the thicker solid curve shows the solution selected according to the action criterion. A new bifurcation occurs at $\mu^* \approx -1.0454$.

that the solution $\mathbf{0}$ is stable for $\mu < \mu_0 = 0$ and unstable for $\mu > \mu_0$. At $\mu_1 \approx -1.2344$, a subcritical bifurcation occurs and one pair of new steady-state solutions appear. We will call \mathbf{u}_+ the upper branch and \mathbf{u}_l the lower branch. The upper branch \mathbf{u}_+ is linearly stable and the lower branch \mathbf{u}_l is linearly unstable. At μ_0 , we have a transcritical bifurcation or exchange of (linear) stability between the lower branch \mathbf{u}_l and the solution $\mathbf{0}$. These bifurcations are summarized in the first subplot of figure 2. Figure 3 shows the phase space of the corresponding ODE system with $\mu = -1$.

Our primary interest here is to compare which one of the two linearly stable solutions \mathbf{u}_+ and $\mathbf{0}$ is more stable if the system is perturbed by noise. We will see that this gives rise to a point of first-order phase transition.

Let us pick two particular values of μ : $\mu = -1.1$ and -1.0 and integrate system (4.1) with a step function as the initial condition. As figure 4 shows, in both cases a travelling wave indeed emerges as the system evolves (further numerical tests do confirm that the system does evolve to travelling waves). The state $\mathbf{0}$ eventually wins when $\mu = -1.1$, but \mathbf{u}_+ takes over at $\mu = -1.0$.

Next, let us examine the cost of going from one state to the other under the action of noise. To do this, we apply the minimum action method [24, 25] to calculate the action and

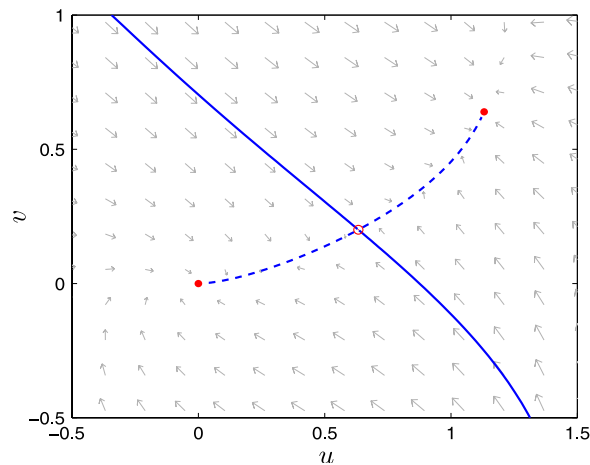


Figure 3. The phase space of the ODE system for (4.2) with the parameter $\mu = -1$. The solid curve is the basin boundary which separates the two stable fixed points (marked with big dots). The broken curve is the unstable manifold of the saddle point (marked with a circle).

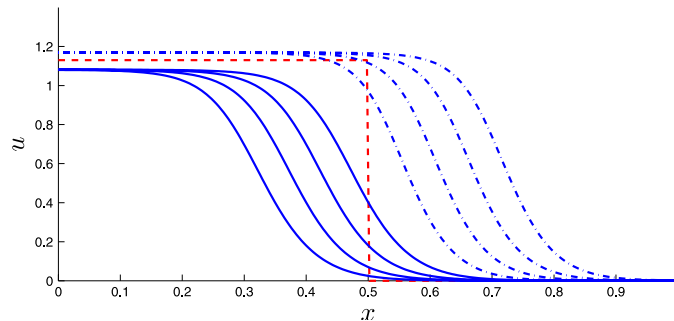


Figure 4. Travelling waves at two different values of μ . The initial condition is a step function with a jump at $x = 0.5$. The solid curves are for $\mu = -1.1$ and the dashed-dotted curves are for $\mu = -1.0$. The travelling wave velocities are $c = -0.084$ and $c = 0.061$, respectively.

the minimum action paths for transitions between u_+ and $\mathbf{0}$ in a large but finite system with space-time white noise and periodic boundary condition. Set $\delta = 0.03$ and $\Omega = [0, 1]$. Let $h(\mu) = Q(u_+; \mu) - Q(\mathbf{0}; \mu)$. Our calculations show that $h(\mu = -1.1) = 0.388 - 1.192 = -0.804$ and $h(\mu = -1.0) = 1.223 - 0.470 = 0.753$. As the system size is further increased, the qualitative picture remains the same.

Both viewpoints suggest that there must be a critical value between $\mu = -1.1$ and $\mu = -1.0$, where the two locally stable states in the spacial extended system exchange their stability properties (see the second subplot in figure 2). *A priori*, the critical values obtained from the two different criterion need not be the same. We calculated both the travelling velocity $c(\mu)$ and the action difference $h(\mu)$ for various values of μ and the results are shown in figure 5.

By examining the point where $c(\mu)$ or $h(\mu)$ changes sign, we identified that the critical value μ^* in both cases is around -1.0454 . This value appears to be robust at large system sizes or small values of δ . The above observation suggests that although a subcritical bifurcation appears at the point μ_1 , in a large system and in the presence of a small noise, the trivial solution $\mathbf{0}$ continues to prevail until μ reaches μ^* .

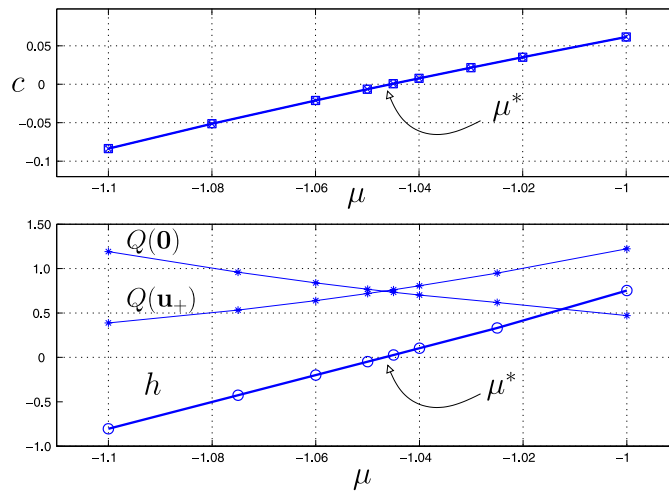


Figure 5. Bifurcation diagram obtained using the 2nd (top) and 1st criteria (bottom). In the first criterion, bifurcation occurs when the function h changes sign. In the second criterion, bifurcation occurs when the velocity of the travelling wave changes sign. The roots of $c(\mu) = 0$ and $h(\mu) = 0$ are both around -1.0454 . $Q(u_+)$ and $Q(0)$ are the escape actions from u_+ and 0 , respectively. $h = Q(u_+) - Q(0)$.

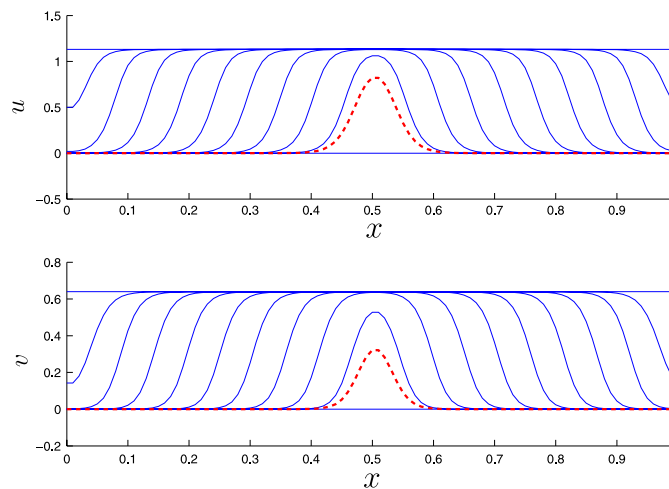
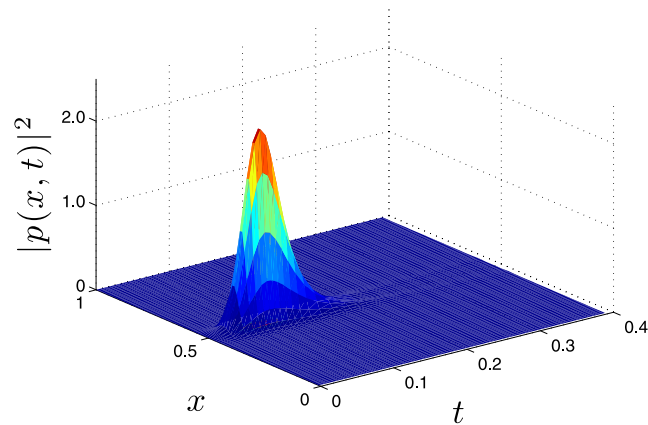
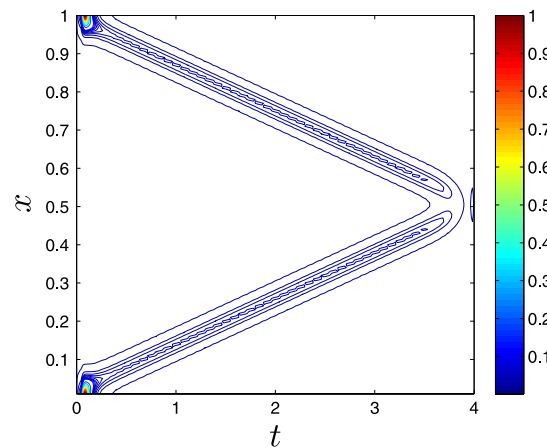


Figure 6. The minimum action path at different times ($\mu = -1.0$, $\delta = 0.01$, $T = 4$ in the minimum action method). Dashed curves show the nucleus, i.e. the saddle point.

We now examine the mechanism of the noise-induced transition from one stable state to another in some detail. Large deviation theory tells us that the most probable transition path is the minimum action path, i.e. the minimizer of (2.10). Let us fix $\mu = -1.0$ and $\delta = 0.01$. We already know that the solution u_+ is more stable than the rest state 0 . The path starting from 0 and ending at u_+ is plotted in figure 6. The dashed curve in figure 6 is the profile of the saddle point. We also note that from that point on, going to the end state u_+ does not require the help from the noise—all the cost is associated with the transition from 0 to the saddle point. A good indicator of the contributions of the noise during the transition process is the term $p(x, t) := \mathcal{F}u(x, t)$ which is defined in



(a) Transition from $\mathbf{0}$ to \mathbf{u}_+ . The contribution from the noise is only needed before nucleation.



(b) Transition from \mathbf{u}_+ to $\mathbf{0}$.

Figure 7. The contribution of the noise ($|p|^2 := |\mathcal{F}u(x, t)|^2$ in (2.7)) plotted with respect to space and time. $\mu = -1.0$. $\delta = 0.01$.

(2.7): $\mathcal{F}u(x, t) = \dot{u}(x, t) - \delta \Delta u(x, t) - \delta^{-1} f(u(x, t))$. The first plot in figure 7 shows the spatial-temporal behaviour of the term $\|p(x, t)\|^2$ for the transition process from $\mathbf{0}$ to \mathbf{u}_+ . In this calculation $T = 4$ but we only show the result in the time interval from 0 to 0.4 to highlight the localized peak near $x = 0.5$ and the time interval around $(0, 0.2)$. Such a peak reveals the contribution of the noise during the nucleation process.

The above picture is the same as what happens in gradient systems. In addition, as we can clearly see, the saddle point solution is in the form of a critical nucleus. Therefore the overall transition takes place via nucleation and propagation, which is the classical mechanism associated with gradient systems. The fact that propagation is a natural consequence of the deterministic dynamics is also consistent with the result of the second criterion.

Similarly one can examine the minimum action path from \mathbf{u}_+ to $\mathbf{0}$ to find that at this parameter value of μ , it is much harder to destabilize the state \mathbf{u}_+ by noise, since it has to work constantly to fight against the tendency for the deterministic dynamics to recover \mathbf{u}_+ . The snapshots of the transition path in this case look almost the same as figure 6, but in a *reversed*

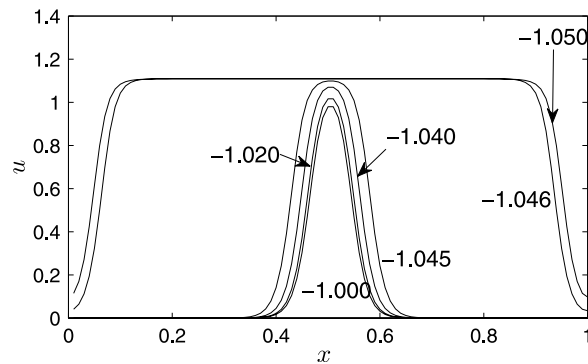


Figure 8. The profiles of the saddle points for the example (4.2) ($\delta = 0.01$). From inside to outside, the values of μ are -1.000 , -1.020 , -1.040 , -1.045 , -1.046 , and -1.050 , respectively.

order, i.e. the noise ‘bends down’ the solution u_+ near two ends at $x = 0, 1$ and continues to ‘squeeze’ the portion of u_+ state from the two ends to the middle in physical space until the system reaches the critical nucleus (red dashed curve). Contribution from the noise can be examined more quantitatively from figure 7(b) which shows contour curves of $\|p(x, t)\|^2$ in the $x-t$ space.

The first-order phase transition discussed above can be further verified by our third criterion about the localized saddle points and the direct Monte Carlo simulation. To this end, the gentlest ascent dynamics (GAD) [26] is used to search for the saddle points. Figure 8 shows the profiles of the u -component of the saddle points associated with various values of μ from -1.000 to -1.050 , computed using the gentlest ascent dynamics. It is clear to see from this figure that from -1.045 to -1.046 , the profile suddenly changes from a local nucleus in the background of $\mathbf{0}$ to being a local nucleus in the background of u_+ . We have verified that this qualitative change also occurs in a larger system with $L = 4$. According to the saddle point criterion, the trivial state $\mathbf{0}$ starts to lose as the bifurcation parameter μ increases from -1.046 to -1.045 . This is consistent with the conclusions drawn from the other two criteria. The agreement of the three criteria for this particular example is due to the fact that the localized saddle point is exactly the transition state for the noise-induced transition path and the travelling wave guarantees that such local saddle point is the only relevant unstable structure for the transition process.

As a way of checking directly these claims, we performed simulation of the noisy system. Figure 9 presents the scatter plot of a long trajectory $(u(\cdot, \cdot), v(\cdot, \cdot))$ for a value of μ which is slightly bigger than the subcritical bifurcation point μ^* . One can see that most points are scattered around the u_+ state.

Even though the example considered is a non-gradient system, its dynamics under noisy perturbations is very much similar to that of the gradient system. The nucleation and propagation picture applies. There is a critical nucleus. The critical nucleus from the less stable state to the more stable state is effectively compact.

5. An example illustrating co-existence

The second example we are going to consider is from [27] where it was used to study the pitchfork bifurcation of the travelling fronts by the singular perturbation analysis. The nonlinearities

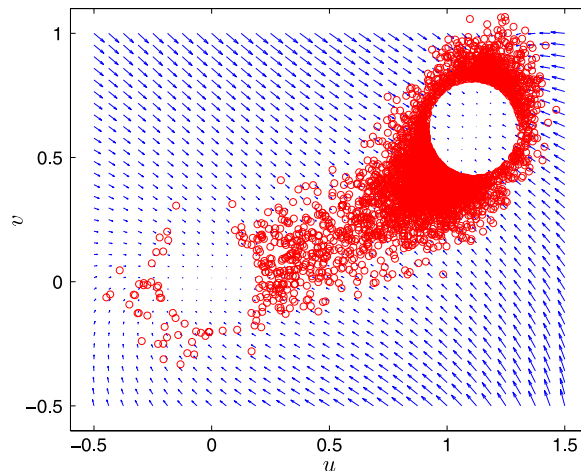


Figure 9. Scatter plot of the solution (u, v) at all spatial-temporal grid points, t from 0 to 1000, time increment is 10. The parameters are $L = 1$, $\mu = -1.044$, $\delta = 0.01$, and noise level $\varepsilon = 0.28$. Only data points outside the disks with radius 0.2 near two base states are shown.

f and g in this example are

$$\begin{aligned} f(u, v) &= \frac{1}{\tau} \left(\frac{1}{2} + u \right) \left(\frac{1}{2} - u \right) \left(u - \frac{1}{2}v \right), \\ g(u, v) &= u - v + \mu. \end{aligned} \quad (5.1)$$

Figure 10 shows the phase plane of the corresponding ODE system. Here $\tau > 0$ is a small parameter, hence the reaction rates for the two components are disparate. The introduction of the additional time scale τ to (5.1) brings in some interesting features; see [27–29] and the references therein. Note that this example has a symmetry: the system is invariant under the transformation: (u, v, μ) to $(-u, -v, -\mu)$. Therefore a first-order phase transition between the two homogeneous states, if exists, must occur at $\mu^* = 0$.

To study the bifurcation for the parameter μ , we fix the small parameter $\tau = 0.02$ in (5.1) and $\delta = 0.04$ in (4.1) but allow the parameter μ to change between $-1/2$ and $1/2$. For all $\mu \in (-1/2, 1/2)$, there are three spatially homogeneous stationary states in this system: two are stable fixed points $\mathbf{u}_{\pm} = (u_{\pm}, v_{\pm}) = (\pm 1/2, \pm 1/2 + \mu)$ and one is a saddle point $(\mu, 2\mu)$.

We first study the travelling front solutions by picking different initial states to evolve the deterministic reaction–diffusion system. Fix $\tau = 0.02$ and $\mu = 0.02$, we choose two different initial conditions (red solid curve and red dash curve as shown in figure 12(a)). It is found that the ‘solid’ initial condition propagates to the left to form a travelling front solution with a negative velocity while the ‘dashed’ initial condition propagates to the right to form a different travelling front solution corresponding to a positive travelling velocity. This situation is illustrated in figure 11 between $-\mu^{\dagger}$ and μ^{\dagger} (μ^{\dagger} to be defined below) where the stable front solutions with both the positive and negative velocities c exist. Now we increase $\mu = 0.03$ and keep other parameters and initial conditions fixed. As one can see from figure 12(b), although the time evolution of the ‘solid’ initial condition remain qualitatively the same, the one for the ‘dashed’ initial condition cannot propagate to the right forever. Instead after a transient propagation, the solution stops and then reflects back to converge to a travelling front solution with a negative velocity. This case corresponds to the region of $|\mu| > \mu^{\dagger}$ in figure 11.

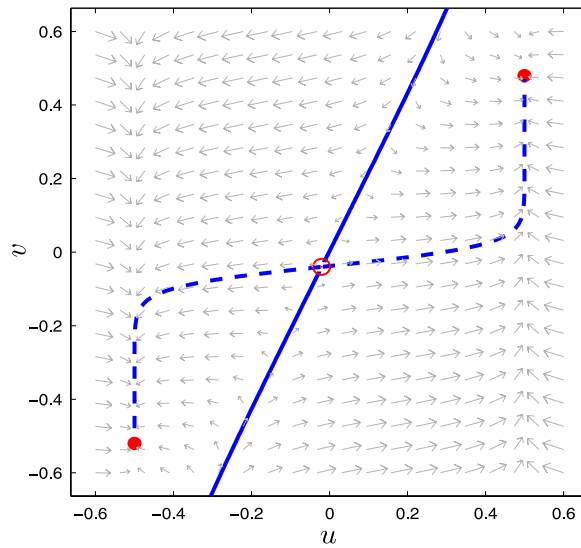


Figure 10. The phase space of the ODE system for (5.1) with the parameter $\mu = -0.03$. The annotation is the same as in figure 3.

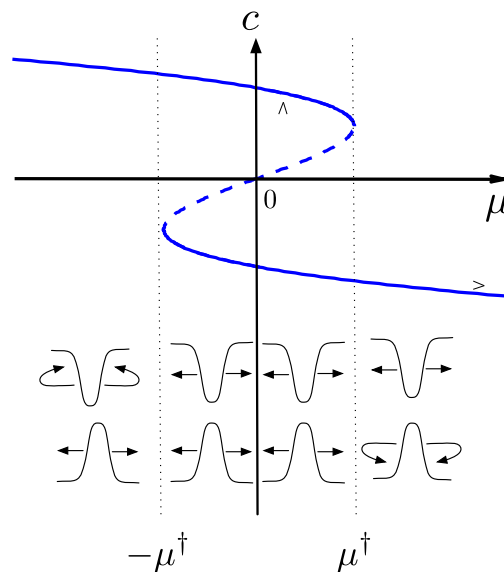


Figure 11. Schematic plot of the bifurcation diagram for the speed c of the travelling front solutions with respect to the parameter μ while the parameter τ is fixed. The solid lines stand for stable travelling front solutions while the dashed for unstable ones. The existence of the pair of index-1 saddles u_{\pm}^s as well as their one-dimensional unstable manifolds (arrow directions) is also illustrated. The meanings of arrows are explained in text. The bifurcation point μ^{\dagger} depends on τ .

The above numerical observation suggests the existence of a bifurcation point μ^{\dagger} . Indeed, according to the results of asymptotic analysis in [27] and the above numerical experiments, we can draw qualitatively a bifurcation diagram in figure 11 for the travelling fronts. By studying the problem using various different domain size ($L = 1, 2, 4$), we identified the value of μ^{\dagger} to be stably around 0.024 when $\tau = 0.02$, $\delta = 0.04$.

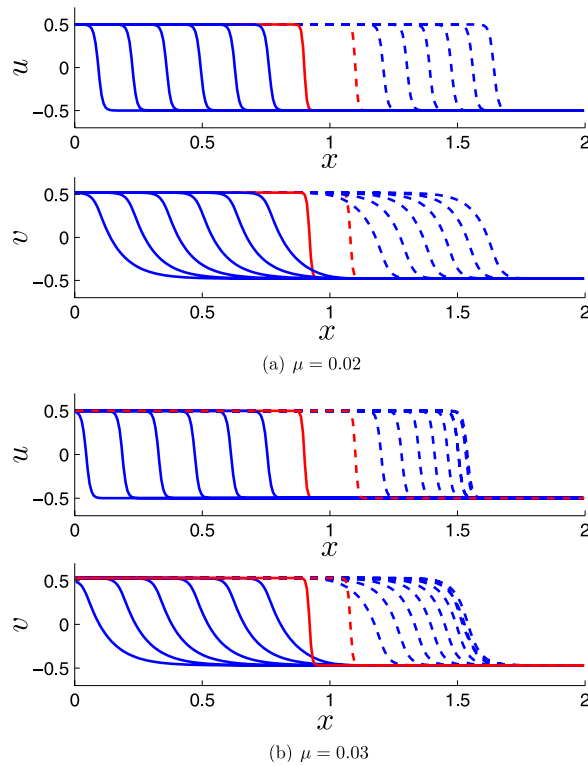


Figure 12. Travelling fronts for two different values of μ ($\tau = 0.02$ and $\mu^\dagger \approx 0.024$). The snapshot of solutions at different times are plotted from *two* different initial conditions (in red, shown in solid and dashed curves, respectively). The solid curves show a front propagating to the left and have negative travelling velocity c while the dashed curves show a front propagating to the right and thus have positive c . Note that at $\mu = 0.03$, the right-travelling front ceases to propagate at a location near $x = 1.6$ and eventually reflects back to u_- .

Obviously, the co-existence of propagating solutions with u_+ invades u_- and with u_- invades u_+ in this system renders our second criterion—i.e. the space competition criterion—discussed in the last section inapplicable.

Next, we study the saddle points in this system in an infinitely long channel. Consider the following system on the semi-infinite line $x \in (0, +\infty)$:

$$\begin{aligned} 0 &= \delta^2 u'' + \frac{1}{\tau} \left(u + \frac{1}{2}\right) \left(\frac{1}{2} - u\right) \left(u - \frac{1}{2}v\right), \\ 0 &= \delta^2 v'' + (u - v + \mu), \end{aligned}$$

where $''$ stands for ∂_x^2 . At $+\infty$ the solution is required to approach one of the base state u_\pm . We first take $u_- = (u_-, v_-)$, i.e. $u(+\infty) = u_-, v(+\infty) = v_-$. The condition at $x = 0$ is $u'(0) = v'(0) = 0$. After the change of variables $u - u_- \rightarrow u, v - v_- \rightarrow v$ and the rescaling $x/\delta \rightarrow x$, the problem becomes

$$\begin{aligned} 0 &= \tau u'' + u(1 - u)(\beta_- + u - \frac{1}{2}v), \\ 0 &= v'' + u - v, \end{aligned} \tag{5.2}$$

with boundary conditions $u'(0) = v'(0) = 0, u(+\infty) = v(+\infty) = 0$, where $\beta_- = -\frac{1}{4} - \frac{1}{2}\mu$. For small τ , there is a boundary layer for the u -component near $x = 0$ and it has a width $O(\sqrt{\tau})$.

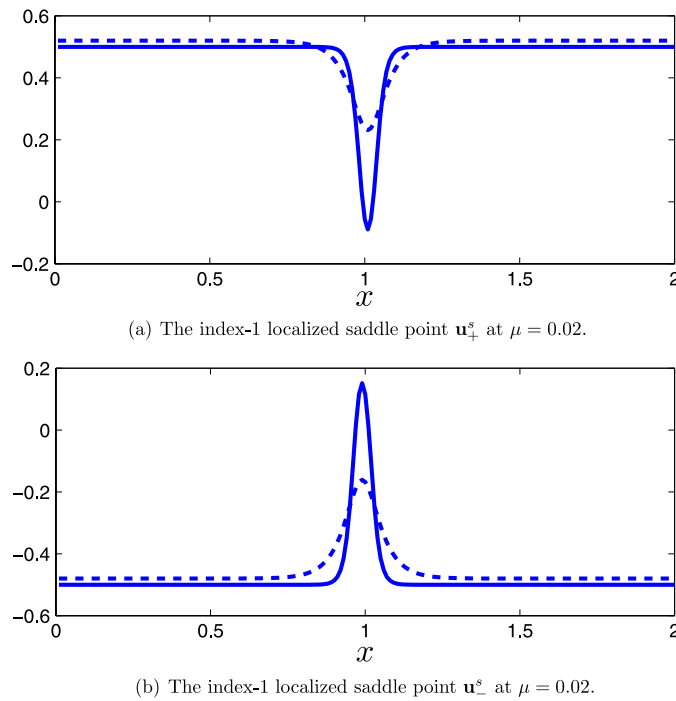


Figure 13. Index-1 localized saddle points at $\mu = 0.02$ (solid and dotted curves are u - and v -component, respectively). There is little change in the profiles of these localized solutions when $L = 1, 2, 4, 8$.

Letting $u(x) = u_0(x/\sqrt{\tau}) + \sqrt{\tau}u_1(x/\sqrt{\tau}) + O(\tau)$, (5.2) gives the leading order problem for u_0 :

$$u_0'' - f'(u_0) = 0,$$

with the boundary condition $u_0'(0) = 0$ and $u_0(+\infty) = 0$. Here

$$f(u) = \frac{1}{4}u^4 + \frac{\beta_- - 1}{3}u^3 - \frac{\beta_-}{2}u^2$$

is a double-well potential function: under the condition $-1/2 < \beta_- < 0$, i.e. $-1/2 < \mu < 1/2$, $f(u)$ has two local minima $u = 0$ and $u = 1$ and $f(1) < f(0)$. Thus, there exists some point \bar{u} between 0 and 1 such that $f(\bar{u}) = f(0)$ and $u(x)$ will go to 0 as $x \rightarrow +\infty$ if it starts from \bar{u} at $x = 0$ with zero velocity $u'(x) = 0$. This means that for all $\mu \in (-1/2, 1/2)$, asymptotically as $\tau \rightarrow 0$, there exists a localized saddle point u_0 which converges to u_- at infinity. Further asymptotic analysis for the v -component shows that v_0 behaves like $v_0 \sim O(\sqrt{\tau})u_0$.

For the homogeneous state u_+ , we can perform the same asymptotic analysis and find another localized saddle point which converges to u_+ at infinity. For nonzero but small τ (i.e. finite domain size), our numerical results confirmed the co-existence of these localized saddle points. The numerical results of these localized saddle points u_{\pm}^s at $\tau = 0.03$ and $\mu = 0.02$ are shown in figure 13. These are index-1 saddle points, i.e. the dynamics has only one unstable direction at these saddle points. Note that these saddles u_{\pm}^s exist for all $\mu \in (-1/2, 1/2)$.

The existence of bifurcation point μ^\dagger for the travelling fronts, which is illustrated in figure 12, implies that there is a corresponding bifurcation of the unstable manifold of the index-1 saddle u_{\pm}^s in the phase space. For $|\mu| < \mu^\dagger$, the unstable manifolds of u_{\pm}^s can reach

Table 1. The ‘nucleation action’ in both directions $u_+ \leftrightarrow u_-$ as μ increases from 0 to 0.05.

μ	$u_+ \rightarrow u_+^s$	$u_- \rightarrow u_-^s$
0	1.34445e-2	1.34445e-2
0.010	1.28793e-2	1.40301e-2
0.020	1.23239e-2	1.46256e-2
0.030	1.17816e-2	1.52346e-2
0.040	1.12526e-2	1.58571e-2
0.050	1.07367e-2	1.64932e-2

both u_+ and u_- . For instance, the saddle u_+^s , which is illustrated in the first row at the bottom of figure 11, has a heteroclinic orbit connecting u_+ in the phase space, which appears in the physical space as the direct invasion of the homogeneous state u_+ . The second heteroclinic orbit is from u_+^s to u_- , corresponding to the propagation of the solution to generate more and more of the u_- state. Such a propagation corresponds to the arrows straightly pointing outward in figure 11. Consequently, the noise-driven system can start from u_+ , grow to a nucleus u_+^s (with help from noise) and then propagate to the whole domain to generate the homogeneous state u_- . In contrast to our first example in section 4, the distinctive feature of this example here is that the above claim of nucleation and propagation can also be made when the initial state is u_- because of the existence of another localized saddle u_-^s for the *same* set of parameters.

For $|\mu| > \mu^\dagger$, if one tracks the unstable manifold of the saddle, say u_+^s , it is found that infinitesimal linear perturbations in the tangent unstable manifold of u_-^s all eventually send the solution back to the homogeneous state u_+ following two routes. One is the same as in the case of $|\mu| < \mu^\dagger$: the direction invasion of u_+ (which is not shown in figure 11) while another involves a transient propagation initially and then eventually an invasion of u_+ (which is illustrated as the hook arrows in figure 11). Such transient behaviour is already seen in figure 12(b). In neither route can the saddle u_+^s reach u_- since the traditional propagation route to u_- is blocked. This means that the localized index-1 saddles u_\pm^s are not the only transition states relevant to the noise-induced transition between u_\pm .

The co-existence of the localized saddles u_+^s and u_-^s renders it impossible to apply the third criterion—saddle point criterion. This leaves us with only one option, the first criterion. Table 1 shows the numerical results of the *nucleation action*—the action required to take the system from the base state to the nucleus. Note that this is not necessarily the escape action defined earlier.

For $|\mu| < \mu^\dagger$, the nucleation action is the true value of the total action between u_\pm (i.e., Q defined in (3.1), section 2). Figure 14 shows a nucleation-propagation type of minimum action path at $\mu = 0.02$. For $|\mu| > \mu^\dagger$, the nucleation action is only a *lower* bound of the escape action between u_\pm , since extra action is needed from the nucleus to the final state. From table 1, $Q(u_+; \mu)$ decreases in μ and $Q(u_-; \mu)$ increases in μ . Therefore, according to our action criterion, u_- is relative more stable than u_+ as $\mu > 0$ and u_+ is relative more stable than u_- as $\mu < 0$.

However, in contrast to the previous example, in the regime when $|\mu| < \mu^\dagger$, the escape actions for both the u_+ state and the u_- state stay finite as the domain size increases, due to the presence of effectively finite sized critical nucleus for both states. Even though the values of the escape actions are different, none of the states will be completely dominant in the thermodynamic limit, no matter how small the noise is, i.e. the two states must co-exist. More precisely, in the thermodynamic limit, the volume fraction of states close to u_+ and u_-

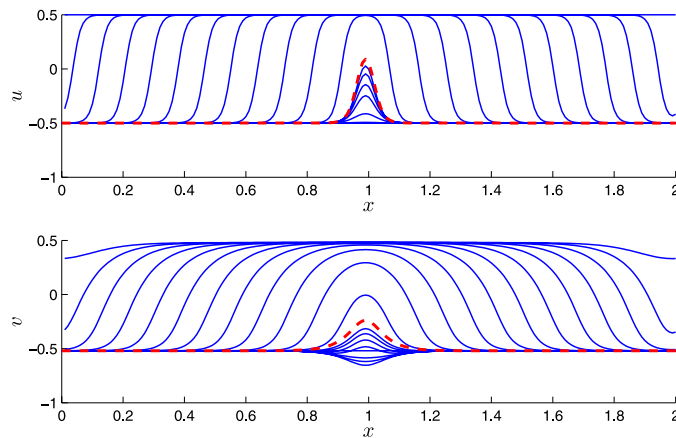


Figure 14. The transition path from u_- to u_+ that passes through u^s (dashed curve). $\mu = 0.02$, $\tau = 0.02$.

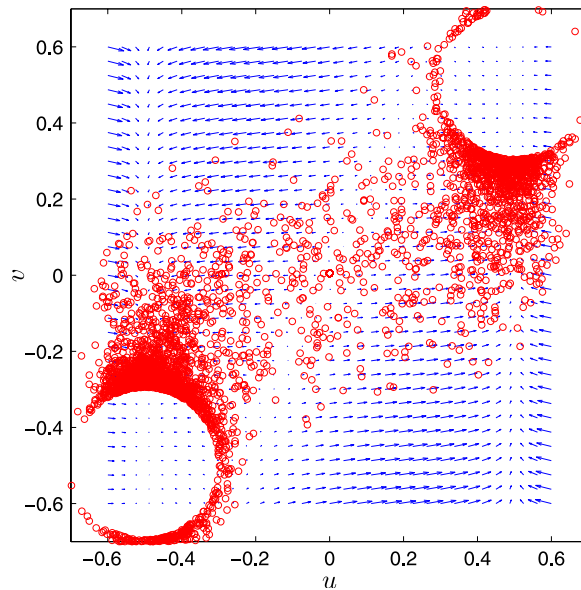


Figure 15. The scatter plot of (u, v) . $L = 1$, $\mu = 0.005$, $\tau = 0.02$, $\delta = 0.04$.

will both converge to finite values, as ε approaches 0. In fact, suppose this is not the case, and only one (homogeneous) state survives in the thermodynamic limit. In the presence of noise, no matter how small, there is always a finite probability of creating a critical nucleus and these nuclei will survive and propagate out, until critical nuclei in the opposite direction appear. Therefore one cannot have homogeneous states in this regime. Direct Monte Carlo simulation (figure 15) of the stochastic PDE with small noise confirms this prediction.

In summary, by comparing the escape action, we can find out which state is more stable. However, whether the less stable states will be suppressed in the thermodynamic limit depends on how the escape action changes with system size. We have shown two examples that give rise to two different situations. In the first example, the difference in the escape action increases,

presumably linearly, with system size. In this case, only the more stable state survives in the thermodynamic limit. In the second example, the difference in the escape action stays bounded as the system size increases. As a result, the two states co-exist.

6. Discussions

We have proposed a theory for noise-driven subcritical instabilities. In a spatially extended system, the background state becomes unstable to small noisy perturbations when the cost (or action) for escaping the domain of attraction of the background state is finite, independent of the system size. Such a system will spontaneously lose its stability. We have also demonstrated the possible existence of a mixed state in which two (homogeneous) states co-exist in a non-gradient system.

Noise-driven subcritical instabilities exhibit interesting finite size effects. For supercritical bifurcations, there is not going to be any significant finite size effects as long as the size of the system is bigger than the wavelength of the most unstable modes. For noise-driven subcritical instabilities, however, if the volume of the system is V , then the probability for the base state to survive is proportional to α^V for some number α between 0 and 1. This means that its life time decreases exponentially as a function of the system size. Finite size systems should also exhibit interesting hysteresis effects. We will postpone the quantitative discussion of this issue to a later paper.

References

- [1] Drazin P G and Reid W H 1981 *Hydrodynamic Stability* (Cambridge: Cambridge University Press)
- [2] Eckhardt B, Schneider T M, Hof B and Westerweel J 2007 Turbulence transition in pipe flow *Annu. Rev. Fluid Mech.* **39** 447–68
- [3] Pomeau Y 1986 Front motion, metastability and subcritical bifurcations in hydrodynamics *Physica D* **23** 3–11
- [4] Gunton J D and Droz M 1983 *Introduction to the Dynamics of Metastable and Unstable States (Lecture Notes in Physics vol 183)* (Berlin: Springer)
- [5] Manneville P 2009 Spatiotemporal perspective on the decay of turbulence in wall-bounded flows *Phys. Rev. E* **79** 025301
- [6] Fife P C 1976 Pattern formation in reacting and diffusing systems *J. Chem. Phys.* **64** 554–64
- [7] Freidlin M I and Wentzell A D 1998 *Random Perturbations of Dynamical Systems (Grundlehren der Mathematischen Wissenschaften) 2 edn* (New York: Springer)
- [8] Touchette H 2009 The large deviation approach to statistical mechanics *Phys. Rep.* **478** 1–69
- [9] Varadhan S 1984 *Large Deviations and Applications (CBMS-NSF Regional Conference Series in Applied Mathematics vol 46)* (Philadelphia: Society for Industrial and Applied Mathematics)
- [10] Faris W G and Jona-Lasinio G 1982 Large fluctuations for a nonlinear heat equation with noise *J. Phys. A: Math. Gen.* **15** 3025–55
- [11] Da Prato G and Zabczyk J 1992 *Stochastic Equations in Infinite Dimensions (Encyclopedia of Mathematics and Its Applications vol 44)* (Cambridge: Cambridge University Press)
- [12] Kohn R V, Otto F, Reznikoff M G and Vanden-Eijnden E 2007 Action minimization and sharp-interface limits for the stochastic Allen–Cahn equation *Commun. Pure Appl. Math.* **60** 393–438
- [13] Sowers R B 1992 Large deviations for a reaction–diffusion equation with non-Gaussian perturbations *Ann. Probab.* **20** 504–37
- [14] Kautz R L 1987 Activation energy for thermally induced escape from a basin of attraction *Phys. Lett. A* **125** 315–9
- [15] Kautz R L 1988 Thermally induced escape: the principle of minimum available noise energy *Phys. Rev. A* **38** 2066–80
- [16] Kautz R L 1994 Quasipotential and the stability of phase lock in nonhysteretic josephson junctions *J. Appl. Phys.* **76** 5538–44
- [17] Graham R 1973 Statistical theory of instabilities in stationary nonequilibrium systems with applications to lasers and nonlinear optics *Quantum Statistics in Optics and Solid-State Physics* ed G Hohler (*Springer Tracts in Modern Physics* vol 66) (Berlin: Springer) p 197
- [18] Graham R 1973 Generalized thermodynamic potential for the convection instability *Phys. Rev. Lett.* **31** 1479–82

- [19] Graham R 1989 Macroscopic potentials, bifurcations and noise in dissipative systems *Noise in Nonlinear Dynamical Systems vol.1: Theory of Continuous Fokker–Planck Systems* ed F Moss and P V E McClintock (Cambridge: Cambridge University Press) pp 225–78
- [20] W E 2011 *Principle of Multiscale Modeling* (Cambridge: Cambridge University Press)
- [21] Matkowsky B and Schuss Z 1982 Diffusion across characteristic boundaries *SIAM J. Appl. Math.* **42** 822
- [22] Maier R S and Stein D L 1993 Escape problem for irreversible systems *Phys. Rev. E* **48** 931–8
- [23] Zhou X 2009 Noise-induced transition pathway in non-gradient systems *PhD Thesis* (Princeton, NJ: Princeton University Press)
- [24] W E, Ren W and Vanden-Eijnden E 2004 Minimum action method for the study of rare events *Commun. Pure Appl. Math.* **57** 637–56
- [25] Zhou X, Ren W and W E 2008 Adaptive minimum action method for the study of rare events *J. Chem. Phys.* **128** 104111
- [26] W E and Zhou X 2011 The gentlest ascent dynamics *Nonlinearity* **24** 1831–42
- [27] Ei S I, Ikeda H and Kawana T 2008 Dynamics of front solutions in a specific reaction–diffusion system in one dimension *Japan J. Indust. Appl. Math.* **25** 117–47
- [28] Rinzel J and Terman D 1982 Propagation phenomena in a bistable reaction–diffusion system *SIAM J. Appl. Math.* **42** 1111–37
- [29] Mimura M 2003 *Reaction–diffusion Systems Arising in Biological and Chemical Systems: Application of Singular Limit Procedures (Lecture Notes in Mathematics vol 1812)* (Berlin: Springer) pp 89–121